Age-associated decline in Nrf2 signaling and associated mtDNA damage may be involved in the degeneration of the auditory cortex: Implications for central presbycusis

YONGQIN LI[1*], XUEYAN ZHAO[1*], YUJUAN HU[1*], HAIYING SUN[1], ZUHONG HE[1], JIE YUAN[1], HUA CAI[1], YU SUN[1], XIANG HUANG[1], WEN KONG[2] and WEIJIA KONG[1]

Departments of [1]Otolaryngology and [2]Endocrinology, Union Hospital, Tongji Medical College, Huazhong University of Science and Technology, Wuhan, Hubei 430022, P.R. China

Received April 10, 2018; Accepted September 19, 2018

DOI: 10.3892/ijmm.2018.3907

Abstract. Central presbycusis is the most common sensory disorder in the elderly population, however, the underlying molecular mechanism remains unclear. NF-E2-related factor 2 (Nrf2) is a key transcription factor in the cellular response to oxidative stress, however, the role of Nrf2 in central presbycusis remains to be elucidated. The aim of the present study was to investigate the pathogenesis of central presbycusis using a mimetic aging model induced by D-galactose (D-gal) *in vivo* and *in vitro*. The degeneration of the cell was determined with transmission electron microscopy, terminal deoxynucleotidyl transferase-mediated deoxyuridine 5'-triphosphate nick-end labeling staining, and senescence-associated β-galactosidase staining. The expression of protein was detected by western blotting and immunofluorescence. The quantification of the mitochondrial DNA (mtDNA) 4,834-base pair (bp) deletion and mRNA was detected by TaqMan quantitative polymerase chain reaction (qPCR) and reverse transcription-qPCR respectively. Cell apoptosis and intracellular ROS *in vitro* were determined with flow cytometry. The levels of nuclear Nrf2, and the mRNA levels of Nrf2-regulated antioxidant genes, were downregulated in the auditory cortex of aging rats, which was accompanied by an increase in 8-hydroxy-2'-deoxyguanosine formation, an accumulation of mtDNA 4,834-bp deletion, and neuron degeneration. In addition, oltipraz, a typical Nrf2 activator, was found to protect cells against D-gal-induced mtDNA damage and mitochondrial dysfunction by activating Nrf2 target genes *in vitro*. It was also observed that activating Nrf2 with oltipraz inhibited cell apoptosis and delayed senescence. Taken together, the data of the present study suggested that the age-associated decline in Nrf2 signaling activity and the associated mtDNA damage in the auditory cortex may be implicated in the degeneration of the auditory cortex. Therefore, the restoration of Nrf2 signaling activity may represent a potential therapeutic strategy for central presbycusis.

Correspondence to: Dr Wen Kong, Department of Endocrinology, Union Hospital, Tongji Medical College, Huazhong University of Science and Technology, 1277 Jiefang Avenue, Wuhan, Hubei 430022, P.R. China
E-mail: wenly-kong@163.com

Dr Weijia Kong, Department of Otolaryngology, Union Hospital, Tongji Medical College, Huazhong University of Science and Technology, 1277 Jiefang Avenue Wuhan, Hubei 430022, P.R. China
E-mail: entwjkong@hust.edu.cn

*Contributed equally

Key words: aging, mitochondrial DNA, NF-E2-related factor 2, oxidative stress, central presbycusis, auditory cortex

Introduction

Age-associated hearing loss, also referred to as presbycusis, is a complex degenerative disease characterized by hearing impairment (1). Presbycusis is an increasingly important public health concern, affecting 40% of individuals aged between 55 and 74 years old (2). Aging-associated decline in auditory sensitivity may be attributed to degeneration of the central and/or peripheral auditory system (3). Central presbycusis refers to age-associated degeneration in the auditory portion of the central nervous system, which affects the ability to localize the temporal and spatial origins of sounds and impairs speech understanding in noisy environments (4). Unfortunately, the mechanisms underlying these changes remain to be fully elucidated.

The pathogenesis of presbycusis may be defined as the sum of all conditions that lead to decreased hearing sensitivity with advancing age. The cumulative effect of intrinsic and extrinsic factors, including hereditary susceptibility, inflammation, and oxidative stress, are reported to lead to hearing loss (5-9). A heritability estimate indicates that 35-55% of the variance in sensory presbycusis is attributed to the effects of genes (10). Certain candidate genes are well known to be associated with oxidative stress, including manganese superoxide dismutase (MnSOD) (11). In addition, the increase in reactive oxygen species (ROS) generation can lead to a state of chronic inflammation (12). The free radical theory of aging suggested by Denham Harman in 1956 suggested that endogenous reactive oxidants cause cumulative oxidative damage

to macromolecules, resulting in the aging phenotype (13). Age-dependent decreases in antioxidant mechanisms and profound accumulation of ROS are causally linked to various health problems, including cardiovascular disease, diabetes and neurodegenerative diseases. NF-E2-related factor 2 (Nrf2) signaling is key in maintaining antioxidant/oxidant homeostasis and in the defense against ROS through modulation of a diverse set of cytoprotective enzymes, including NAD(P)H quinone oxidoreductase 1 (NQO1), heme oxygenase-1 (HO-1), and MnSOD (14,15), all of which have potent antioxidant properties. Numerous studies have demonstrated that oxidative stress serves a major role in the pathophysiology of presbycusis (16,17). As an upstream regulator of Nrf2, Wnt activation protects against oxidative stress-induced hair cell damage (18). However, whether the Nrf2 pathway is involved in central presbycusis remains to be elucidated.

Mitochondria are important in the aging process (19,20). Presbycusis, as one of the age-associated diseases, has been associated with mitochondrial oxidative damage (21). Although mitochondrial (mt)DNA only encodes 13 mitochondrial proteins, it is crucial for mitochondrial function (22). Due to the proximity of mtDNA to the source of endogenous oxidants and the lack of any protective histone covering, mtDNA is sensitive to oxidative stress (23). An accumulation of mtDNA mutations and/or deletions may lead to mitochondrial dysfunction, further increasing ROS generation and oxidative damage (24). Mutations of mtDNA include the 4,834-base pair (bp) deletion in rats and the 4,977-bp deletion in humans, which are known as common deletions (CDs) and act as an accurate biomarker for aging (25). In our previous studies, it was found that mtDNA deletions may cause sensitivity to environmental stress and aggravate hearing impairment (26). Previous studies have demonstrated that Nrf2 may be involved in the cellular response to oxidative stress and maintenance of mitochondrial function (27,28). However, the underlying association between Nrf2 signaling and mtDNA damage in the process of aging have not been thoroughly examined.

Natural aging can be experimentally modeled by the chronic administration of D-galactose (D-gal). Animals treated with D-gal exhibit increased oxidative stress, dysfunctional mitochondria and neural damage; consequently, these animals exhibit decreased cognitive function similar to the natural aging process (29,30). Our previous studies demonstrated that oxidative stress induced by D-gal may lead to central presbycusis (31,32). The focus of the present study was to investigate the role of Nrf2 signaling in the degeneration of the auditory cortex using a mimetic aging model induced by D-gal. Whether the Nrf2 signaling pathway is involved in mtDNA damage and cell senescence *in vitro* was also investigated.

Materials and methods

Animals. A total of 162 male 4-week-old Sprague-Dawley rats, weighing 89.25±13.60 g, were obtained from the Experimental Animal Center of Tongji Medical College, Huazhong University of Science and Technology (HUST; Wuhan, China). A previous study showed that presbycusis is influenced by gender (33). Males demonstrate a higher incidence of presbycusis with a rapid deterioration in the hearing threshold and anatomical degeneration (33). Therefore, male rats were selected for the experimental model, instead of female rats. All rats were housed in an air-conditioned animal facility (22˚C, 50-60% relative humidity) with a 12:12-h light-dark cycle and allowed free access to standard chow and tap water. Following acclimatization for 4 weeks, the 2-month-old rats were randomly allocated into two groups: The normal saline (NS; n=81) and D-galactose (D-gal; n=81) groups. The rats in the D-gal group were injected subcutaneously with D-gal (500 mg/kg/day; Sigma-Aldrich; Merck KGaA, Darmstadt, Germany) for 8 weeks, whereas rats in the NS group received the same volume of 0.9% normal saline (NS) on the same schedule, injected once a day at a fixed time. Following the final injection, the NS and D-gal groups were divided into three age subgroups: 4-month-old (immediately following the final injection), 10-month-old (6 months following the final injection) and 16-month-old (12 months following the final injection). All procedures involving the care of animals were performed in accordance with the guidelines of the Care and Use of Laboratory Animals of the National Institutes of Health (34). The protocol was approved by the Committee on the Ethics of Animal Experiments of HUST.

Cell culture and treatment. Well-differentiated rat pheochromocytoma (PC12) cells induced by nerve growth factor were obtained from the Shanghai Institutes for Biological Sciences of the Chinese Academy of Cell Resource Center (Shanghai, China). The PC12 cells were maintained and cultured in DMEM (HyClone; GE Healthcare Life Sciences, Logan, UT, USA) supplemented with 10% fetal bovine serum (FBS; Gibco; Thermo Fisher Scientific, Inc., Waltham, MA, USA) and 100 IU/ml penicillin (Sigma-Aldrich; Merck KgaA) at 37˚C in a humidified atmosphere of 95% air and 5% CO_2. Target-specific Nrf2 small interfering (si)RNAs (GenePharma; Shanghai, China) were designed to knock down the gene expression in PC12 cells. An siRNA encoding a nonsense sequence was designed as the negative control. The cells were transfected in 2 ml Opti-MEM (Gibco; Thermo Fisher Scientific, Inc.) containing 10 μl Lipofectamine™ 2000 (Invitrogen; Thermo Fisher Scientific, Inc.), with 200 nM Nrf2 siRNA or control siRNA according to the manufacturer's protocol. The Opti-MEM medium was replaced 6 h later with DMEM containing FBS. The following siRNA was used to knock down the expression of Nrf2: siRNA-Nrf2, sense 5'-GCAAGAAGCCAGAUACAAATT-3' and antisense 5'-UUUGUAUCUGGCUUCUUGCTT-3'; control, sense 5'-UUCUCCGAACGUGUCACGUTT-3' and antisense 5'-ACGUGACACGUUCGGAGAATT-3'. The cells were incubated with D-gal (Sigma-Aldrich; Merck KGaA) at 37˚C in a humidified atmosphere containing 5% CO_2 for 48 h, with or without oltipraz (Sigma-Aldrich; Merck KGaA) pretreatment for 1 h. Dimethyl sulfoxide (DMSO; Sigma-Aldrich; Merck KgaA) was used for the dissolution of oltipraz. The DMSO groups were pretreated with an equal volume of DMSO (<0.2% final).

Measurements of malondialdehyde (MDA) levels. The level of MDA in the auditory cortex of rats (n=6/subgroup) was determined using a colorimetric kit (Nanjing Jiancheng Bioengineering Institute, Nanjing, China) according to the manufacturer's protocol.

Terminal deoxynucleotidyl transferase-mediated deoxyuridine 5'-triphosphate nick-end labeling (TUNEL) staining. The combination of ketamine and chlorpromazine can be used for anesthesia in rats (35,36). In the present study, the rats (n=6/subgroup) were anesthetized with a combination of ketamine (100 mg/kg) and chlorpromazine (5 mg/kg) via intraperitoneal injection, according to our previous studies (37,38). Following deep anesthesia determined by respiratory, palpebral reflex, pedal withdrawal reflex, and cutaneous reflex (39,40), the animals were transcardially perfused with 400 ml of saline followed by 4% paraformaldehyde solution (pH 7.2-7.4). Following perfusion, the brain was dissected from the skull, and the auditory cortex was separated and immersed overnight in the same fixative. The right side was prepared for TUNEL staining and the left side was prepared for immunofluorescence. The following processes were performed, as previously described (41). Apoptosis in the auditory cortex of rats was detected using a TUNEL assay (Roche Diagnostics GmbH, Mannheim, Germany) according to the manufacturer's protocol. DAPI staining solution (1 μg/ml; Beyotime Institute of Biotechnology, Haimen, China) was used to counterstain the nuclei. The labeled cells were detected with a laser scanning confocal microscope (Nikon Corporation, Tokyo, Japan).

DNA extraction and quantification of the mtDNA 4,834-bp deletion. Following deep anesthesia, the rats (n=6/subgroup) were sacrificed. The brain was dissected from the skull and both sides of the auditory cortex were obtained from each subgroup. All removed tissue was frozen in a refrigerator (Siemens AG, Munich, Germany) at -80˚C. The right side was prepared for mtDNA analysis; the left side was prepared for RNA analysis. Total DNA was extracted from 20 mg of tissue in the auditory cortex or 10^7 cultured cells utilizing a Genomic DNA Purification kit (Tiangen Biotech Co., Ltd., Beijing, China) according to the manufacturer's protocol. The percentages of CDs were determined by TaqMan quantitative polymerase chain reaction (qPCR) assays. As the D-Loop region is rarely deleted, it serves as the conservative segment. The PCR primers and probes for the mtDNA CD (4,834-bp deletion) and mtDNA D-loop were as previously described (42). The sequences used were as follows: D-Loop, probe 5'-TTGGTTCATCGTCCA TACGTTCCCCTTA-3', forward 5'-GGTTCTTACTTCAGG GCCATCA-3' and reverse 5'-GATTAGACCCGTTACCAT CGAGAT-3'; Common deletion sequences, probe 5'-TCACTT TAATCGCCACATCCATAACTGCTGT-3', forward 5'-GAT TAGACCCGTTACCATCGAGAT-3' and reverse 5'-CGAAGT AGATGATCCGTATGCTGTA-3'. PCR amplification was performed using an LC-480 real-time PCR system (Roche Diagnostics GmbH) in a 20-μl reaction volume consisting of 10 μl of a 2X TaqMan PCR mix (Takara Bio, Inc., Dalian, China), 0.2 μl of each probe (10 mM), 0.4 μl of each forward and reverse primer (10 mM), 5 μl of distilled water, and 4 μl of the sample DNA (10 ng/ml). The amplification conditions were as follows: 30 sec at 95˚C then 40 cycles of 10 sec at 95˚C and 30 sec at 60˚C. ΔCq ($Cq_{deletion}$-$Cq_{D\text{-}loop}$) was used to reflect the abundance of the mtDNA 4,834-bp deletion. The relative expression indicating the factorial difference in the deletions between the experimental group and control group was calculated using the $2^{-\Delta\Delta Cq}$ method (43), where $\Delta\Delta Cq=\Delta Cq_{\text{mtDNA deletion in experimental group}}-\Delta Cq_{\text{mtDNA deletion in control group}}$.

RNA extraction and reverse transcription-qPCR (RT-qPCR) analysis. Total RNA was extracted from ~50 mg of tissue or 10^7 cultured cells with an RNA extraction kit (Omega Bio-tek, Inc., Norcross, GA, USA) according to the manufacturer's protocol. The cDNA was reverse transcribed using the PrimeScript RT reagent kit (Takara Bio, Inc.). Fold changes in respective gene expression were calculated by normalizing to the level of the house-keeping gene GAPDH. The primer sequences designed for RT-qPCR analysis are shown in Table I. PCR amplification was performed in an LC-480 real-time PCR system (Roche Diagnostics GmbH) in a 20-μl reaction volume consisting of 10 μl 2X SYBR Green II PCR Master Mix (Takara Bio, Inc.), 1 μl each forward and reverse primer, 6 μl distilled water and 2 μl the sample cDNA. The amplification conditions were as follows: 95˚C for 5 min; 45 cycles of 95˚C for 10 sec, 60˚C for 20 sec and 72˚C for 20 sec; followed by 95˚C for 5 sec and 65˚C for 60 sec. The relative mRNA expression was calculated using the $2^{-\Delta\Delta Cq}$ method.

Transmission electron microscopy (TEM). Following anesthesia, the rats (n=3/subgroup) were perfused transcardially with 0.9% oxygenated saline, followed by 2.5% glutaraldehyde in 0.1 M phosphate buffer (pH 7.2-7.4). Following perfusion, the auditory cortex was isolated and immersed overnight in the same fixative solution. *In vitro*, following the indicated treatments, the cells were collected and immersed in the fixative solution overnight. The following processes were performed, as described in our previous study (41). The sections (60-100 nm) were analyzed with a FEI TecnaiG^{2}20 TWIN microscope (Thermo Fisher Scientific, Inc.) at x1,700, x3,500, and x6,500 magnification.

Immunofluorescence. The processes of immunofluorescence were as described in our previous study (37). The primary antibodies included anti-kelch-like ECH-associated protein 1 (keap1; 1:100; cat. no. ab150654; Abcam, Cambridge, MA, USA), anti-8-hydroxy-2'-deoxyguanosine (8-OHdG; 1:200; cat. no. sc-393871; Santa Cruz Biotechnology, Inc., Dallas, TX, USA), and anti-Nrf2 (1:200; cat. no. ARG53382; Arigo Biolaboratories, Hamburg, Germany). The secondary antibodies included FITC-labeled donkey anti-rabbit IgG (H+L) (1:200; cat. no. ANT024; AntGene Biotechnology, Inc., Wuhan, China) and FITC-labeled donkey anti-mouse IgG (H+L) (1:200; cat. no. ANT023; AntGene Biotechnology, Inc.). Fluorescent images were visualized with a laser scanning confocal microscope (Nikon Corporation). The quantification of immunofluorescence was performed using ImageJ 10.0 software (National Institutes of Health, Bethesda, MD, USA).

Western blot analysis. Following deep anesthesia, six rats from each subgroup were sacrificed. The tissue of the auditory cortex was prepared for western blot analysis. The protein expression levels of cleaved caspase-3 and cytochrome *c* in the auditory cortex and PC12 cells were determined using western blot analysis. Preparation of the cytosolic and mitochondrial fractions was performed using a commercially available cytosol/mitochondria fractionation kit (Beyotime Institute of Biotechnology) according to the manufacturer's protocol. The proteins were extracted using RIPA lysis buffer (Beyotime Institute of Biotechnology), which contained a

Table I. Primer sequences for polymerase chain reaction analysis.

Gene	Direction	Primer sequence	Accession no.
NQO1	Forward	5'-GGGGACATGAACGTCATTCTCT-3'	NM_017000.3
	Reverse	5'-AGTGGTGACTCCTCCCAGACAG-3'	
HO-1	Forward	5'-TGTCCCAGGATTTGTCCGAG-3'	NM_012580.2
	Reverse	5'-ACTGGGTTCTGCTTGTTTCGCT-3'	
MnSOD	Forward	5'-ATGTTGTGTCGGGCGGCGTGCAGC-3'	NM_017051.2
	Reverse	5'-GCGCCTCGTGGTACTTCTCCTCGGT-3'	
GAPDH	Forward	5'-GCAAGTTCAACGGCACAG-3'	NM_017008.4
	Reverse	5'-GCCAGTAGACTCCACGACAT-3'	

NQO1, NAD(P)H quinone oxidoreductase 1; HO-1, heme oxygenase-1; MnSOD, manganese superoxide dismutase.

cocktail of phosphatase inhibitor and phenylmethylsulfonyl fluoride, following the manufacturer's protocol. Protein concentrations were determined using an Enhanced BCA Protein Assay kit (Beyotime Institute of Biotechnology). Equal quantities of protein (30 μg) were loaded onto 12% SDS-polyacrylamide gels for electrophoresis, separated and transferred to polyvinylidene difluoride membranes (EMD Millipore, Billerica, MA, USA). The membranes were incubated in blocking solution [5% non-fat milk (BD Biosciences, Franklin Lakes, NJ, USA) in Tris-buffered saline] for 1 h at room temperature. Subsequently, the membranes were incubated overnight at 4˚C with the following primary antibodies: Anti-cleaved caspase-3 (1:200; cat. no. 9661; Cell Signaling Technology, Inc., Danvers, MA, USA) and anti-cytochrome *c* (1:500; cat. no. ab13575; Abcam). The following processes were performed as previously described (37). Quantification of the western blot results was performed using ImageJ 10.0 software (National Institutes of Health) to measure the intensities of the bands.

Determination of mitochondrial membrane potential ($\Delta\Psi m$). Cell $\Delta\Psi$m was detected using a Mitochondrial Membrane Potential Assay kit with JC-1 (Beyotime Institute of Biotechnology) according to the manufacturer's protocol. Briefly, the cells were seeded in 24-well plates at a density of $1x10^4$ cells per well. Following the indicated treatments, the cells were incubated with JC-1 stain and incubated at 37˚C for 20 min. The cells were then washed three times with phosphate-buffered saline (PBS) and immediately analyzed with a confocal laser-scanning microscope (Nikon Corporation).

Cell viability test. Cell viability was assessed with the Cell Counting Kit-8 (CCK-8) assay (Dojindo Molecular Technologies, Inc., Kumamoto, Japan) according to the manufacturer's protocol. Briefly, the cells were seeded on a 96-well plate and left to attach overnight. Following the indicated treatments, 10 μM of the CCK-8 solution was dissolved in serum-free medium and added to each well of the plates, and the plates were incubated for 30 min at 37˚C. The absorbance at 450 nm was quantified on an automated microplate reader (Bio-Tek Instruments, Inc., Winooski, VT, USA).

Senescence-associated β-galactosidase (SA-β-gal) staining assay. SA-β-gal is one of the best-characterized and reliable methods for measuring senescence *in vitro* and *in vivo*, by measuring the activity of β-Gal expressed by senescent cells through immunohistochemistry (44). The number of senescent cells was evaluated using a Senescence β-Galactosidase Staining kit (Beyotime Institute of Biotechnology) according to the manufacturer's protocol. Briefly, following the indicated treatments, the cells were washed with PBS at least three times and then fixed in fixative solution for 15 min at room temperature. The fixed cells were washed with PBS, stained by β-Gal staining solution and incubated at 37˚C overnight. Under a light microscope (Olympus Corporation, Tokyo, Japan), the presence of blue granules in the cytoplasm was considered as a positive result for β-Gal staining, reflecting senescence of the examined cells.

Flow cytometry. Intracellular ROS generation was detected using 2',7'-dichlorodihydrofluorescein diacetate (DCFH-DA; Beyotime Institute of Biotechnology). Briefly, following treatment, the PC12 cells were incubated with 10 μM DCFH-DA for 30 min at 37˚C. The cells ($1x10^6$) were then suspended in PBS and examined by flow cytometry (FACSCalibur; BD Biosciences). Apoptosis in the cells was also evaluated using Annexin V/propidium iodide (PI) staining (BD Biosciences) followed by flow cytometry, according to the manufacturer's protocol.

Statistical analysis. All data are shown as the mean ± standard deviation. Analyses were performed using GraphPad Prism 6 software (GraphPad Software, Inc., San Diego, CA, USA). Two-tailed, unpaired Student's t-tests were used to determine statistical significance when comparing two groups, and one-way analysis of variance followed by a Dunnett's multiple comparisons test was used when comparing more than two groups. $P<0.05$ was considered to indicate a statistically significant difference.

Results

Neurodegeneration in the auditory cortex. To investigate changes in the ultrastructure in the auditory cortex, a TEM assay was used. In the NS groups, neurons of the auditory

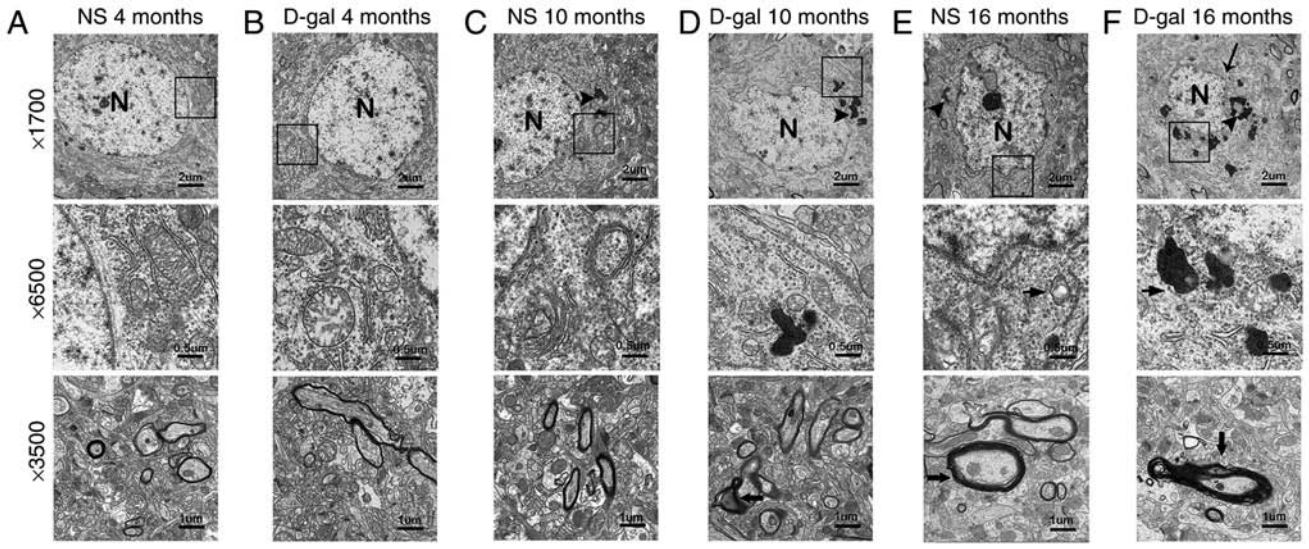

Figure 1. Ultrastructural morphology of the auditory cortex. In the (A) 4-month-old NS group, (B) 4-month-old D-gal group and (C) 10-month-old NS group, the nuclei were round, the chromatin was uniform and the nuclear membrane was intact; the mitochondria were normal and myelin in nerve fibers was intact. In the (D) 10-month old D-gap group, (E) 16-month-old NS group and (F) 16-month-old D-gal group, irregular nuclei, abundant lipofuscin, swollen mitochondria and disrupted myelin were observed. NS, normal saline; D-gal, D-galactose. The arrowheads indicate the lipofuscin; the bold arrows indicates the disrupted myelin; the normal arrows indicate the nuclear membrane; N, nucleus.

cortex exhibited no notable ultrastructural changes in the 4- and 10-month-old rats. In the D-gal groups, the auditory cortex exhibited no notable ultrastructural changes in the 4-month-old rats (Fig. 1A-C). Irregular nuclei, abundant lipofuscin, swollen mitochondria and disrupted myelin were observed in the 16-month-old NS group rats. However, the 10-month-old rats in the D-gal groups exhibited similar ultrastructural changes to those observed in the 16-month-old NS group rats (Fig. 1D and E). These ultrastructural changes were more prominent in the 16-month-old D-gal group rats (Fig. 1F). These results revealed that D-gal treatment accelerates neurodegeneration in the auditory cortex of rats.

Cell apoptosis and MDA levels in the auditory cortex. TUNEL staining was performed to investigate the effects of D-gal and age on cell apoptosis in the auditory cortex. Only low levels of TUNEL-positive cells were found in the 4-month-old NS and the 4-month-old D-gal groups. The number of TUNEL-positive cells in the auditory cortex increased with age in the NS groups. The number of TUNEL-positive cells was significantly increased in the 10- and 16-month-old D-gal groups compared with the age-matched NS groups (Fig. 2A and B). MDA, a byproduct of lipid peroxidation induced by free radicals, is widely used as a biomarker of oxidative stress (45). Therefore, to determine the level of oxidative stress, the levels of MDA in the auditory cortex were measured. Compared with the 4-month-old NS group, the MDA levels were significantly increased in the 16-month-old NS group. In addition, compared with age-matched NS rats, MDA levels in the D-gal-treated rats were significantly increased in the 10- and 16-month-old groups (Fig. 2C). These data suggested that cell apoptosis and oxidative stress levels in the auditory cortex were increased in the D-gal-induced aging rats.

Increased mitochondrial cytochrome c release and cleaved caspase-3 in D-gal-induced aging rats. Cytochrome *c* serves a critical role in the mitochondrial-mediated apoptotic pathway and activation of caspase in mammalian cells. Cleaved caspase-3 is a marker of the activation of apoptosis. As shown in Fig. 3A-C, western blot analysis demonstrated that the release of cytochrome *c* into the cytosolic fraction and cleaved caspase-3 in the auditory cortex of the D-gal-induced mimetic aging group were significantly increased compared with the age-matched control groups. These data suggested that the release of mitochondrial cytochrome c and the level of cleaved caspase-3 in the auditory cortex was increased in the D-gal-induced aging rats.

Formation of 8-OHdG and accumulation of mtDNA CDs in the auditory cortex. The levels of oxidative damage of DNA are typically assessed through biomarkers, including the formation of 8-OHdG (46). The results of the immunofluorescence assays (Fig. 4A and B) revealed that the levels of 8-OHdG in the D-gal group were significantly higher compared with those in the NS group at different ages. Compared with the 4-month-old group, the 8-OHdG levels in the 16-month-old group were markedly increased. In addition, 8-OHdG fluorescence was observed predominantly in the cytoplasm, suggesting that ROS induced mtDNA oxidative damage in the auditory cortex. Mutations in mtDNA, including the 4,834-bp deletion in rats and the 4,977-bp deletion in humans, referred to as CDs, are closely associated with presbycusis (25). TaqMan qPCR analysis was performed to evaluate the accumulation of CDs in the auditory cortex. Consistent with the increase in 8-OHdG levels, CD levels increased with age. Furthermore, CD levels were significantly increased in the D-gal groups compared with those in the age-matched NS groups (Fig. 4C). These results indicated that oxidative damage to mtDNA was increased in the auditory cortex of aging rats.

Age-associated changes of Nrf2 signaling in the auditory cortex. Keap1 is a component of the E3 ubiquitin ligase

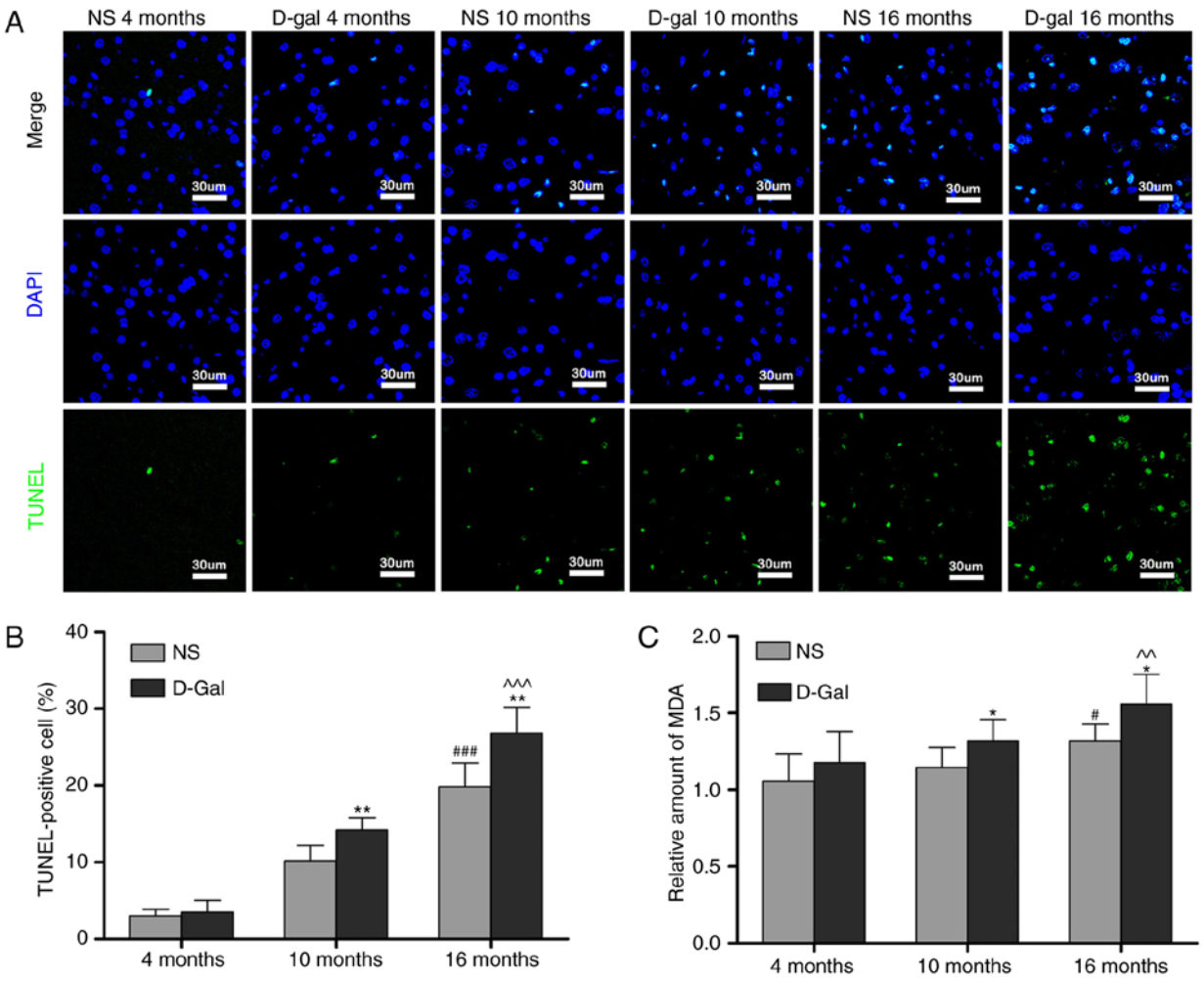

Figure 2. Cell apoptosis and MDA levels in the auditory cortex. (A) Representative images of TUNEL staining. (B) Quantitative assessment of TUNEL-positive cells in the auditory cortex. (C) MDA levels in the auditory cortex. For all experiments, *P<0.05 and **P<0.01, vs. age-matched NS group; $^{\#}$P<0.05 and $^{\#\#\#}$P<0.001 vs. 4-month-old NS group; $^{\wedge\wedge}$P<0.01 and $^{\wedge\wedge\wedge}$P<0.001, vs. 4-month-old D-gal group. The data are presented as the mean ± standard deviation. MDA, malondialdehyde; NS, normal saline; D-gal, D-galactose; TUNEL, terminal deoxynucleotidyl transferase-mediated deoxyuridine 5'-triphosphate nick-end labelling.

complex that targets Nrf2 for degradation (47). The results of the immunofluorescence analysis demonstrated that the protein levels of Keap1 were increased in the 16-month-old NS group, but that the levels of Keap1 in the 16-month-old D-gal group exhibited a more prominent increase. In addition, compared with the age-matched NS groups, the level of Keap1 in the D-gal-treated groups were significantly increased (Fig. 5A and B). To further elucidate the role of the transcription factor Nrf2 in the aging process, the levels of Nrf2 in the auditory cortex were measured by immunofluorescence. Compared with the 4-month-old NS group, the level of Nrf2 was decreased in the 16-month-old NS group. Additionally, compared with the 4-month-old D-gal group, the levels of Nrf2 in the 16-month-old D-gal group exhibited a more marked decrease (Fig. 6A and B). In addition, the decline in nuclear levels of Nrf2 coincided with a significant attenuation in the expression of genes that are constitutively regulated by Nrf2, including NQO1, HO-1 and MnSOD. The transcription of these Nrf2 target genes was quantified by RT-qPCR analysis and gene expression was normalized to GAPDH. The results demonstrated that the mRNA levels of NQO1, HO-1 and MnSOD in the 16-month-old NS group were significantly lower compared with those in the 4-month-old NS group (Fig. 6C-E). Compared with the 4-month-old D-gal group, the mRNA levels of NQO1, HO-1 and MnSOD were significantly decreased in the 16-month-old D-gal group (Fig. 6C-E). Taken together, these results demonstrated that Nrf2 signaling is disrupted in D-gal-induced aging rats.

Oltipraz activates the Nrf2 pathway and increases cellular antioxidant activity in PC12 cells. The PC12 rat pheochromocytoma cell line, a traditional cell line for neuroscience studies, is commonly used in neurobiology and neuropharmacology *in vitro* (48,49). In addition, the PC12 cell line has been widely used as a model to investigate oxidative stress-induced cell injury and senescence (50-52). In the present study, a mimetic aging model induced by D-gal was established in PC12 cells. The cultured PC12 cells were treated with increasing concentrations of D-gal (0-40 mg/ml) for 48 h and cell viability was then evaluated using CCK-8. Cellular activity was altered by treatment with D-gal in a concentration-dependent manner, exhibiting a decreasing pattern that was statistically significant at 20 mg/ml. According to these results (Fig. 7A), 15 mg/ml of D-gal was utilized to induce cell senescence in subsequent

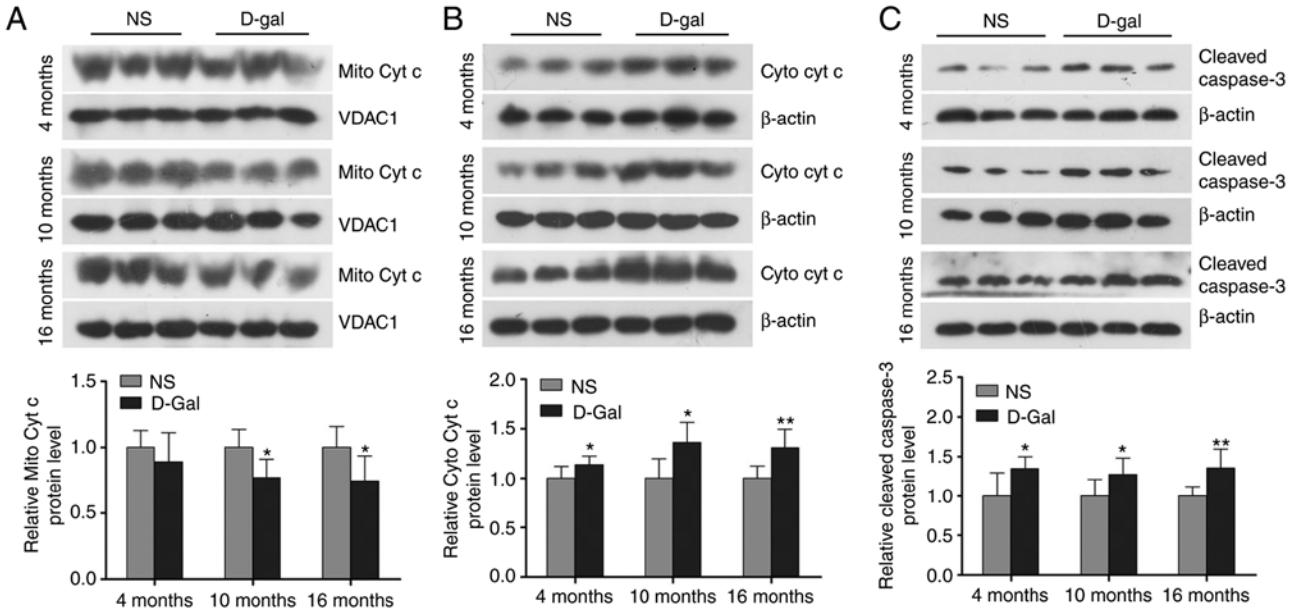

Figure 3. D-gal treatment increases mitochondrial cytochrome *c* release and cleaved caspase-3 in the auditory cortex of rats. (A) Western blot analysis of Cyt c levels in the mitochondrial fraction. (B) Western blot analysis of Cyt c levels in the cytosolic fraction. (C) Western blot analysis of cleaved caspase-3 levels. The relative levels of Mito Cyt c were normalized to VDAC1; the relative levels of Cyto c and cleaved caspase-3 in each group were normalized to β-actin. *P<0.05 and **P<0.01, vs. NS groups. The data are presented as the mean ± standard deviation. Mito Cyt c, mitochondrial cytochrome *c*; Cyto Cyt c, cytosolic cytochrome *c*; NS, normal saline (control) group; D-gal, D-galactose (mimetic aging) group.

experiments. As Nrf2 is an important regulator of redox genes, the downregulation of NQO1, HO-1 and MnSOD genes was observed following Nrf2 knockdown (Fig. 7B-D). The results showed that Nrf2 can regulate the transcription of NQO1, HO-1 and MnSOD genes. To investigate whether the Nrf2 signaling pathway is involved in senescence and mtDNA damage, the PC12 cells were pretreated with oltipraz, which has been found to activate Nrf2, enhance glutathione biosynthesis and increase phase II detoxification enzymes (53). To select an optimal concentration of oltipraz, the PC12 cells were pretreated with this agent at concentrations ranging between 0 and 100 μM for 1 h. The CCK-8 assay indicated that pretreatment with oltipraz protected cells against injury induced by D-gal in a concentration-dependent manner; the maximal cytoprotective effect was observed at 50 μM oltipraz (Fig. 7E). To confirm activation of the Nrf2 pathway by oltipraz, the transcription levels of antioxidant genes NQO1, HO-1 and MnSOD were measured. Oltipraz (50 μM) significantly increased the mRNA levels of NQO1, HO-1 and MnSOD (Fig. 7F). To measure the antioxidant activity of oltipraz, ROS generation in the PC12 cells was assessed using DCFH-DA staining. The increased ROS levels under D-gal treatment were found to be partially attenuated by the addition of oltipraz (Fig. 7G and H). These results demonstrated that activating the Nrf2 pathway with oltipraz can increase cellular antioxidant activity.

Oltipraz protects PC12 cells against D-gal-induced mtDNA oxidative damage, mtDNA CD and mitochondrial dysfunction. It is well established that oxidative stress results in nuclear DNA damage and mtDNA damage when the antioxidant/oxidant equilibrium is disrupted (54). The level of oxidatively damaged DNA is generally measured by the formation of the biomarker 8-OHdG. Oltipraz pretreatment attenuated the formation of 8-OHdG induced by D-gal (Fig. 8A and B). To determine mitochondrial genome integrity, the levels of mtDNA CDs were measured in PC12 cells by TaqMan qPCR and oltipraz was found to decrease the incidence of mtDNA CDs induced by D-gal (Fig. 8C). To investigate whether the Nrf2 signaling pathway is involved in mitochondrial function, the ΔΨm was examined using JC-1. The results demonstrated that oltipraz attenuated the loss of ΔΨm induced by D-gal in PC12 cells (Fig. 8D and E). In addition, D-gal treatment induced the release of cytochrome *c* into the cytosolic fraction and the activation of caspase-3 in PC12 cells, which were partially suppressed by oltipraz pretreatment (Fig. 8F-H). Taken together, these data demonstrated that activating Nrf2 signaling with oltipraz attenuates D-gal-induced mtDNA damage and mitochondrial dysfunction.

Oltipraz attenuates D-gal-induced structural damage, apoptosis and senescence in PC12 cells. To further examine the cytoprotective effect of oltipraz, the ultrastructure of the treated cells was observed by TEM. Cells in the control and DMSO groups did not shown notable ultrastructural changes; however, irregular nuclei and swollen mitochondria were observed in the D-gal group. Notably, these abnormal changes were alleviated in the D-gal group pretreated with oltipraz (Fig. 9A). These data indicated that oltipraz protected the cells from D-gal-induced damage. SA-β-gal is the most widely known biomarker of cellular senescence. To investigate whether the Nrf2 signaling pathway is involved in cell senescence, SA-β-gal staining was performed in PC12 cells and a marked increase in SA-β-gal-positive cells was observed in the D-gal group, which was partially reversed by oltipraz pretreatment (Fig. 9B and C). Annexin V-FITC/PI staining and flow cytometry were used to confirm the anti-apoptotic effect of oltipraz in the D-gal-treated PC12 cells. The rate of apoptosis was increased by D-gal treatment, but this effect

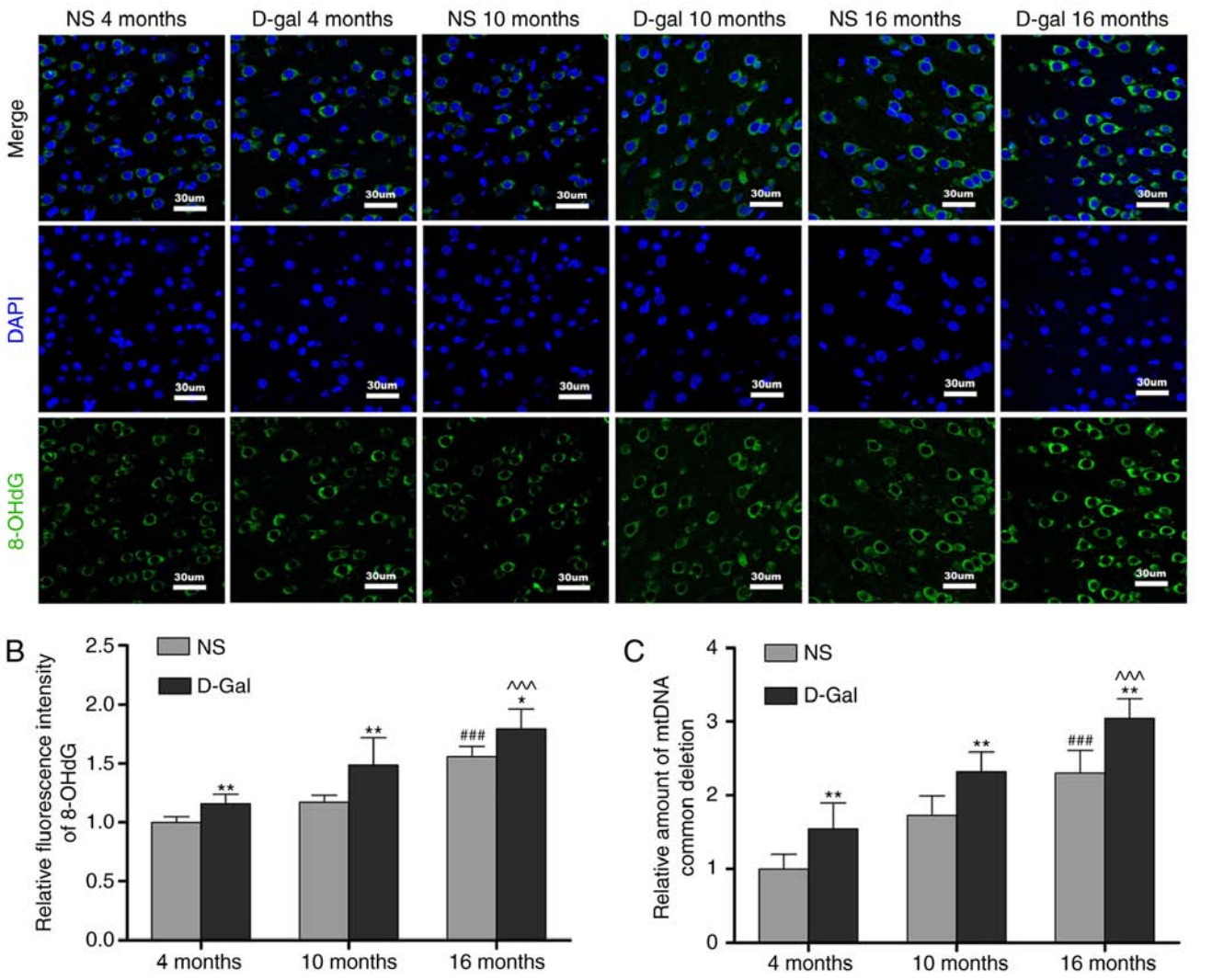

Figure 4. Formation of 8-OHdG and accumulation of mtDNA CDs in the auditory cortex. (A) Representative immunofluorescence images labeled with 8-OHdG in the auditory cortex. (B) Quantitative assessment of 8-OHdG fluorescence intensity in the auditory cortex. (C) Age-associated accumulation of mtDNA CDs in the auditory cortex. For all experiments, *P<0.05 and **P<0.01, vs. the age-matched NS group; $^{###}$P<0.001, vs. 4-month-old NS group; $^{\wedge\wedge\wedge}$P<0.001, vs. 4-month-old D-gal group. The data are presented as the mean ± standard deviation. 8-OHdG, 8-hydroxy-2'-deoxyguanosine; mtDNA, mitochondrial DNA; CD, common deletion; NS, normal saline; D-gal, D-galactose.

was attenuated by pretreatment with oltipraz (Fig. 9D and E). Taken together, these findings demonstrated that oltipraz exerts a protective effect against D-gal-induced cell damage, senescence and apoptosis in PC12 cells.

Discussion

In the present study, apoptosis and abnormal ultrastructural morphology were more prominent with aging in the auditory cortex of the NS groups (Figs. 1 and 2A and B). Specifically, irregular nuclei, abundant lipofuscin, swollen mitochondria and disrupted myelin were observed in the 16-month-old NS group. The lifespan of the majority of Sprague-Dawley rats is 2.5-3 years; thus, the age of 16-months is equivalent to late adulthood in rats (55). The levels of apoptosis and changes in ultrastructure morphology in the 10-month-old D-gal-treated rats were similar to those in the 16-month-old NS rats, but were more pronounced in the 16-month-old D-gal-treated group. Therefore, rats in the 16-month-old D-gal-induced mimetic aging group were classified as being the equivalent of old age. These data indicated that the rat model of aging in the auditory cortex was successfully established using D-gal.

In the present study, the data revealed that MDA levels were significantly elevated in the auditory cortex of the naturally aging and D-gal-induced aging rats (Fig. 2C). MDA is the final product of lipid peroxidation (45), and its accumulation suggests that oxidative stress in the auditory cortex of the aging rat has become severe. Nrf2 signaling is critical in the cellular response to oxidative stress (56). Previous studies in *Caenorhabditis elegans (C. elegans)* demonstrated that the knockdown of SKN-1, the homolog of Nrf2 in *C. elegans*, shortens lifespan (57). A previous study also demonstrated that repression of the Nrf2-mediated antioxidant response is a key contributor to the premature aging phenotype in Hutchinson-Gilford Progeria Syndrome mesenchymal stem cells (58). In the present study, it was observed that the levels of nuclear Nrf2 and Nrf2-regulated antioxidant genes were decreased in the auditory cortex of the aging rats (Fig. 6). The mechanism underlying the downregulation of Nrf2-mediated antioxidant genes in aging is likely multifaceted. Keap1, a

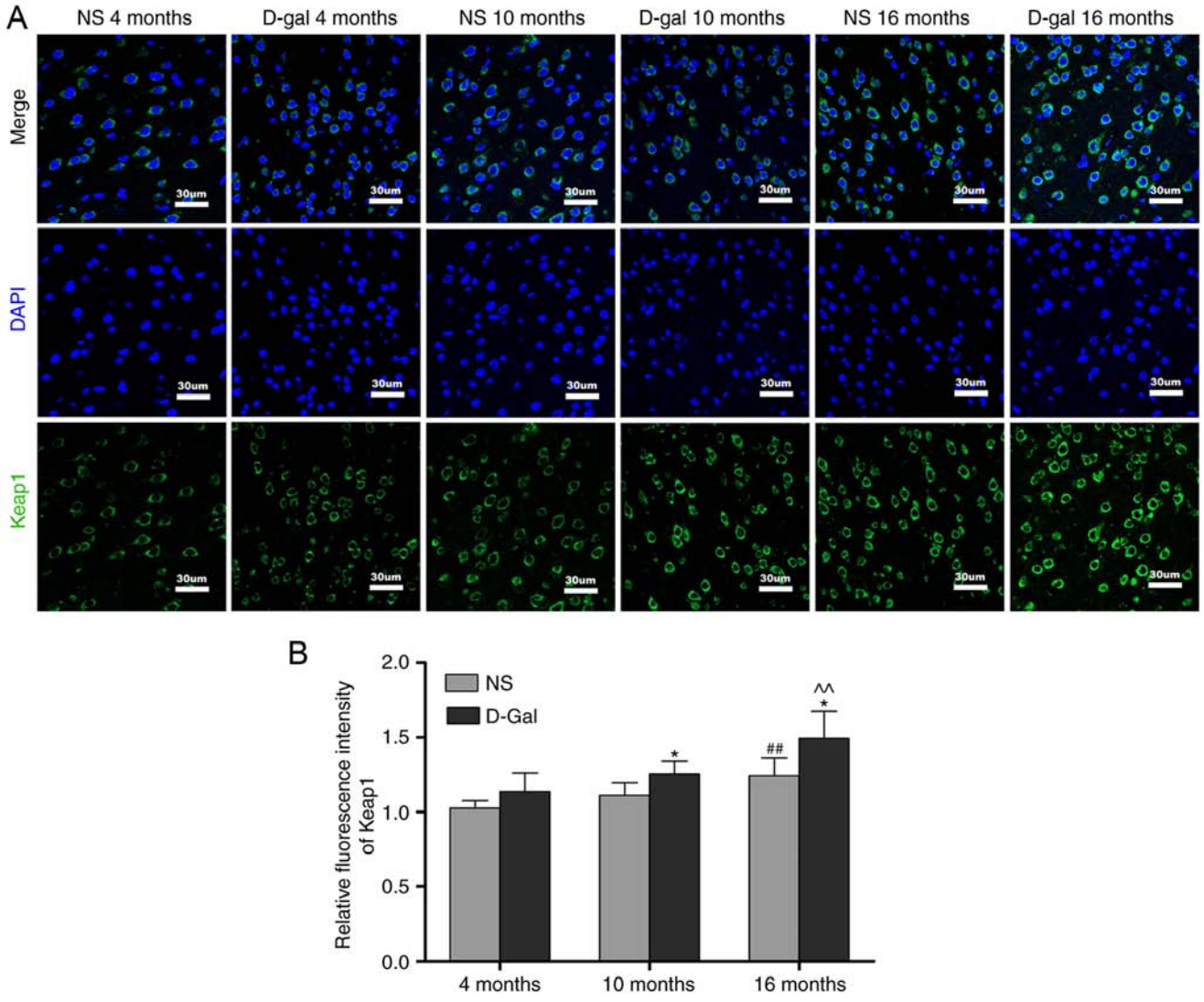

Figure 5. Age-associated changes in Keap1 levels in the auditory cortex. (A) Representative immunofluorescence images labeled with anti-Keap1 in the auditory cortex. (B) Quantitative assessment of Keap1 fluorescence intensity in the auditory cortex. For all experiments, *P<0.05, vs. age-matched NS group; $^{\#\#}$P<0.01, vs. 4-month-old NS group; $^{\wedge\wedge}$P<0.01, vs. 4-month-old D-gal group. The data are presented as the mean ± standard deviation. NS, normal saline; D-gal, D-galactose; Keap1, kelch-like ECH-associated protein 1.

negative regulator of Nrf2, which acts as an adaptor between Nrf2 and the ubiquitination ligase Cullin-3, promotes the degradation of Nrf2 by the proteasome and inhibits the nuclear translocation of Nrf2 (59). The present study demonstrated that the expression of Keap1 was increased in the auditory cortex of the aging rats (Fig. 5A and B). Increased levels of Keap1 and decreased levels of Nrf2 have also been observed in a chronic renal failure rat model (60). Decreased Nrf2 signaling may lead to failure of the cytoprotective system and enhance the sensitivity of cells to oxidative stress. Accordingly, the results of the present study demonstrated that oxidative stress, apoptosis and degeneration in the auditory cortex of aging rats may be associated with the dysregulation of Nrf2 signaling, which may be involved in the pathogenesis of central presbycusis.

Mitochondria are considered to be key in the progression of presbycusis (61). Mammalian mtDNA is critical for mitochondrial function (24), and oxidative damage to mtDNA may be attributed to an excess of ROS and/or inadequate antioxidant defense. One of the major oxidative modifications of DNA is 8-OHdG, which is an oxidative DNA mutagenic lesion that has been directly correlated with the development of pathological processes (62,63). The present study demonstrated that the levels of 8-OHdG in the auditory cortex increased with age (Fig. 4A and B). mtDNA is particularly susceptible to oxidative damage due to several factors; it is in close proximity to the ROS-generating respiratory chain, it is not covered by histones or other DNA-associated proteins, and it lacks a robust repair system compared with that of nuclear DNA (23). Consistent with the other oxidative stress-related degenerative disorders, including Alzheimer's disease, age-related macular degeneration, and diabetic hearts (64-66), the present study showed that 8-OHdG fluorescence was observed predominantly in the cytoplasm of cells, which suggests that mtDNA is the primary target of oxidative damage. In accordance with the increased 8-OHdG levels, the findings of the present study also demonstrated that the accumulation of mtDNA CDs was increased in the aging rats (Fig. 4C). Furthermore, the release of cytochrome *c* into the cytoplasm and cleaved caspase-3 in

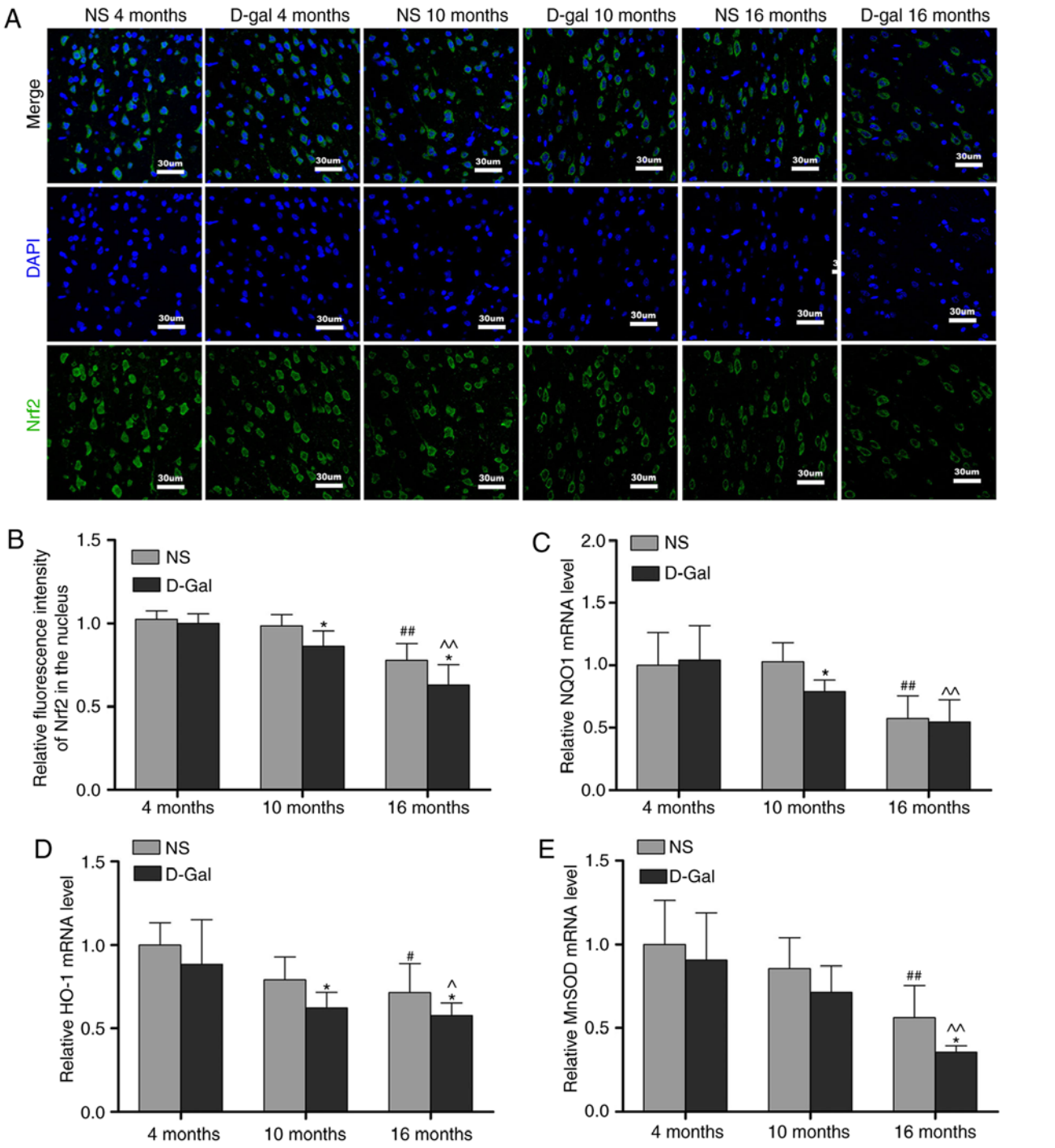

Figure 6. Age-associated decline of Nrf2 signaling in the auditory cortex. (A) Representative immunofluorescence images stained with anti-Nrf2 antibody. (B) Quantitative presentation of the fluorescence intensity of Nrf2 in the nucleus. mRNA levels of (C) NQO1, (D) HO-1 and (E) MnSOD in the auditory cortex. For all experiments, *P<0.05, vs. age-matched NS group; $^{\#}$P<0.05 and $^{\#\#}$P<0.01, vs. 4-month-old NS group; $^{\wedge}$P<0.05 and $^{\wedge\wedge}$P<0.01, vs. 4-month-old D-gal group. The data are presented as the mean ± standard deviation. Nrf2, NF-E2-related factor 2; NQO1, NAD(P)H quinone oxidoreductase 1; HO-1, heme oxygenase-1; MnSOD, manganese superoxide dismutase; NS, normal saline; D-gal, D-galactose.

the auditory cortex of the D-gal-induced mimetic aging group were increased (Fig. 3). These results demonstrated that oxidative damage to mtDNA and mitochondrial stress-associated apoptosis are increased in the auditory cortex of naturally aging and D-gal-induced aging rats. Nrf2 is a transcription factor that regulates a number of antioxidant and cytoprotective genes to protect against ROS-induced toxicity (56). Nrf2-regulated antioxidant enzymes, including NQO1, HO-1 and MnSOD, have potent antioxidant properties. NQO1, an obligatory two-electron reductase, is a ubiquitous cytosolic enzyme that catalyzes the reduction of quinone substrates (67). As an important Nrf2-dependent antioxidant response gene, NQO1 defects result in increased susceptibility to DNA damage in the marrow cells of mice (68). HO-1 catalyzes the oxidative degradation of heme to biliverdin and carbon monoxide; a deficiency in HO-1 may elevate the levels of ROS and superimpose oxidative injury in endothelial cells (69). MnSOD is the main antioxidant enzyme responsible for scavenging superoxide in the mitochondrial

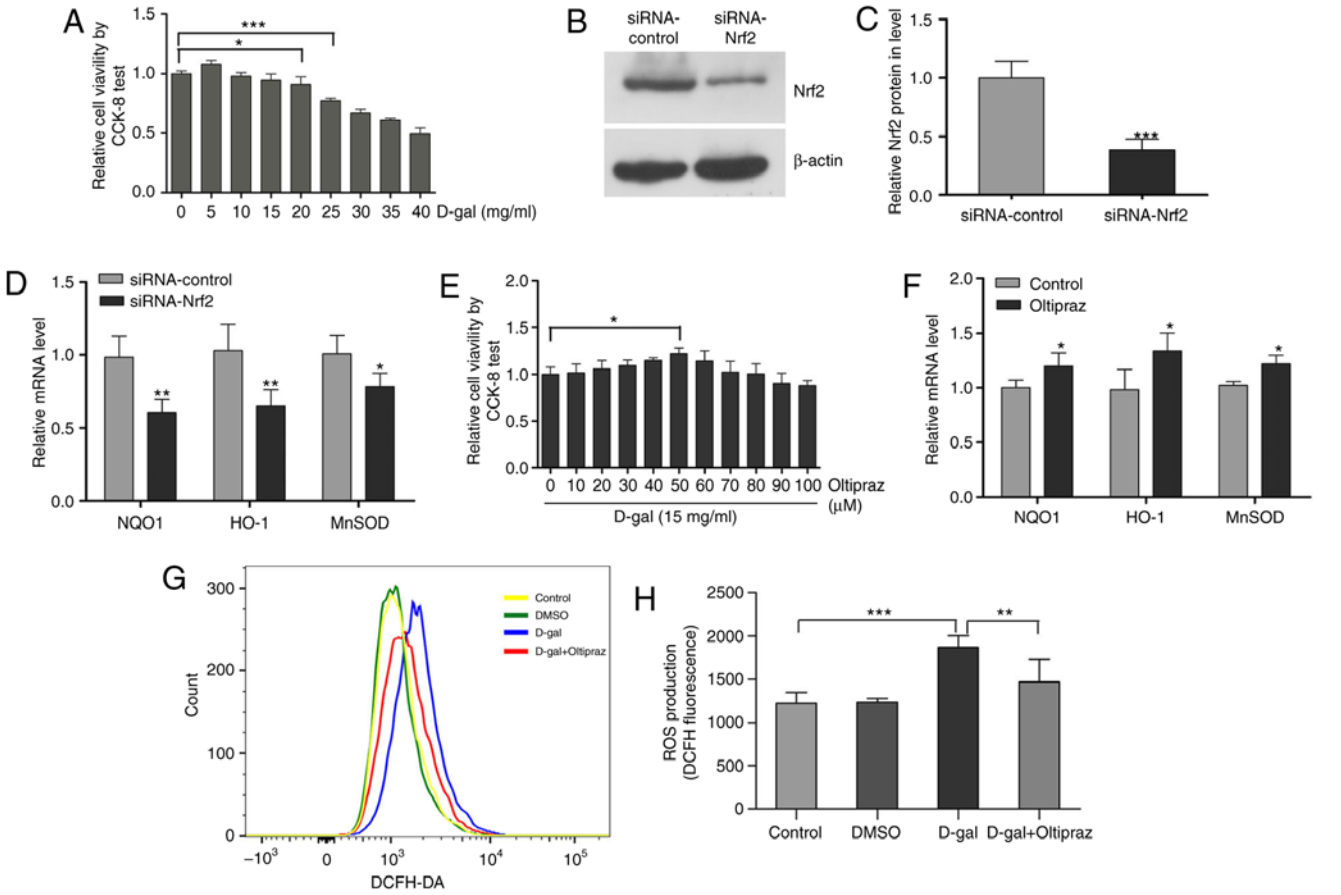

Figure 7. Oltipraz activates the Nrf2 pathway and increases cellular antioxidant activity in PC12 cells. (A) An optimal concentration of D-gal was selected using a CCK-8 test. (B) Protein expression of Nrf2; (C) Nrf2 siRNA transfection decreased the protein expression of Nrf2 in PC12 cells. (D) Nrf2 siRNA transfection decreased the expression of Nrf2 target genes in PC12 cells. (E) A maximal cytoprotective concentration of oltipraz was selected using the CCK-8 test. (F) mRNA levels of NQO1, HO-1 and MnSOD in the control and oltipraz groups. (G) ROS levels were measured in the treated cells using DCFH-DA staining and analyzed by flow cytometry; (H) graph shows ROS levels. For all experiments, *P<0.05, **P<0.01 and ***P<0.001. The data are presented as the mean ± standard deviation. Nrf2, NF-E2-related factor 2; D-gal, D-galactose; siRNA, small interfering RNA; CCK-8, Cell Counting Kit-8; ROS, reactive oxygen species; DCFH-DA, dichlorodihydrofluorescein diacetate; NQO1, NAD(P)H quinone oxidoreductase 1; HO-1, heme oxygenase-1; MnSOD, manganese superoxide dismutase; DMSO, dimethyl sulfoxide.

matrix. It has been reported that decreased mitochondrial function and increased mtDNA oxidative damage, including that by 8-OHdG, are observed in the liver of MnSOD$^{+/-}$ mice (70). In the present study, it was demonstrated that the expression levels of Nrf2-dependent antioxidant genes (NQO1, HO-1 and MnSOD) were downregulated in the auditory cortex of aging rats (Fig. 6C-E). It is likely that age-associated attenuation of the antioxidant defense system in the auditory cortex, potentially due to disruption of Nrf2 signaling, increases the sensitivity of mtDNA to oxidative damage and leads to the development of a 'vicious cycle', in which oxidative damage to mtDNA leads to further mitochondrial dysfunction and oxidant generation. Taken together, the findings of the present study, in addition to those of previous studies, suggested that mtDNA damage in the auditory cortex may be associated with Nrf2 signaling disruption during aging.

To further confirm the involvement of the Nrf2 pathway in mtDNA damage and aging, PC12 cells were pretreated with oltipraz, which is a typical Nrf2 activator (53). The results demonstrated that oltipraz activated the transcription of Nrf2-regulated antioxidant genes (NQO1, HO-1 and MnSOD) and decreased the D-gal-induced production of ROS in PC12 cells (Fig. 7F-H). Damage to mtDNA and mitochondrial dysfunction are closely associated with aging (24,71). The present study demonstrated that oltipraz attenuated D-gal-induced mtDNA damage and mitochondrial dysfunction (Fig. 8). It is possible that oltipraz upregulated the expression of stress response genes (NQO1, HO-1 and MnSOD) and increased intracellular antioxidant capacity, thus protecting mtDNA against ROS and maintaining mitochondrial function. Onken and Driscoll reported that the activation of SKN-1, the homolog of Nrf2 in *C. elegans*, prolongs the lifespan of *C. elegans* (72). As markers of aging, cell apoptosis and the number of SA-β-gal-positive cells were increased in the D-gal-treated group in the present study, in accordance with our previous studies (73,74). It was also observed that the activation of Nrf2 signaling by oltipraz inhibited apoptosis and delayed the senescence induced by D-gal (Fig. 9). Taken together, these results indicate that the activation of Nrf2 signaling may be important in maintaining mtDNA integrity and delaying aging.

In conclusion, Nrf2 signaling was found to be decreased in the auditory cortex in a rat model of aging. The activation of Nrf2 with oltipraz reduced mtDNA damage and delayed

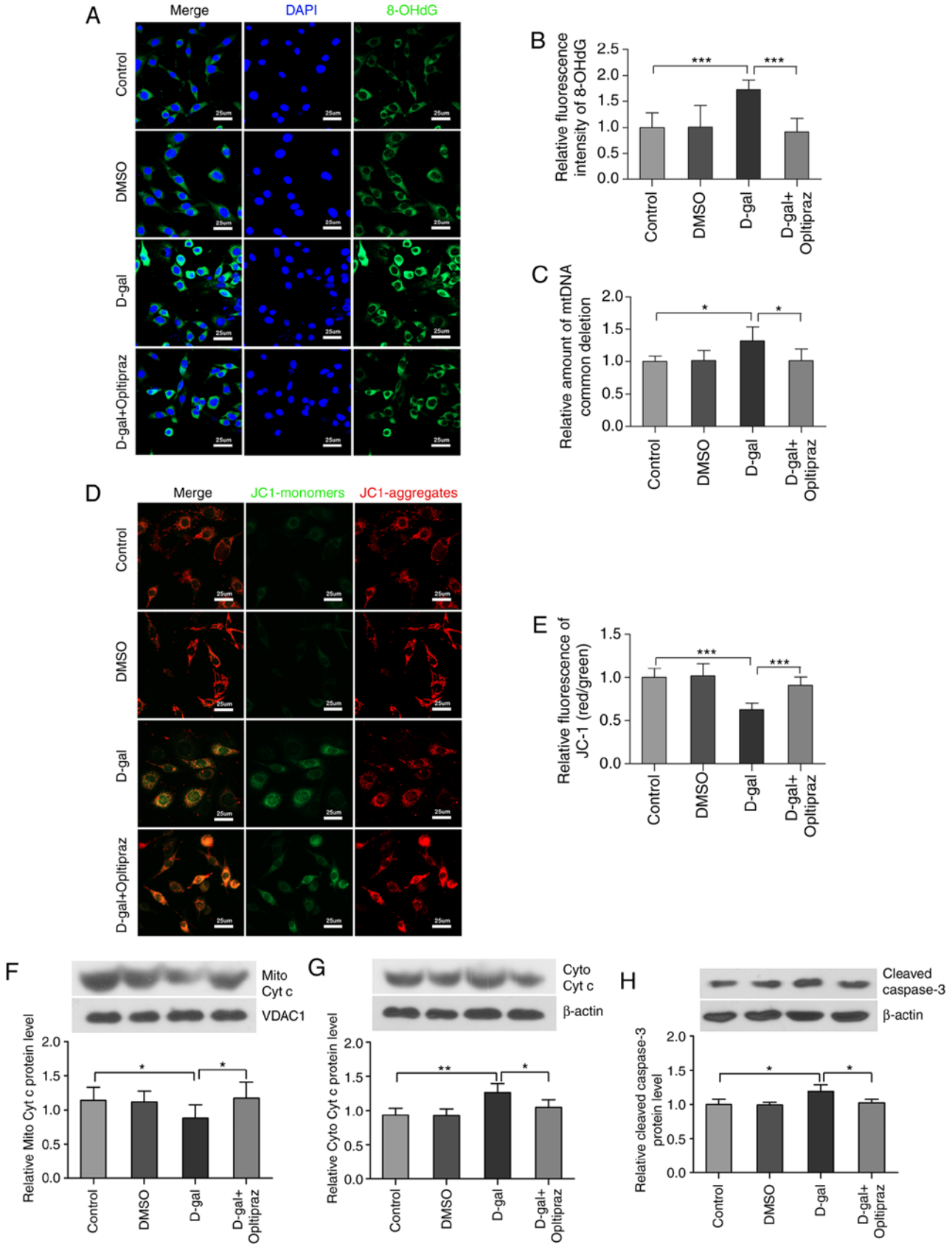

Figure 8. Oltipraz inhibits D-gal-induced 8-OHdG formation, mtDNA CDs and mitochondrial dysfunction. (A) Representative confocal images of 8-OHdG. (B) Quantitative assessment of 8-OHdG fluorescence in the treated cells. (C) Levels of mtDNA CDs in the treated cells were analyzed by TaqMan quantitative polymerase chain reaction. (D) Representative images of JC-1. The red colour indicates the JC-1 aggregate fluorescence from healthy mitochondria, the green colour indicates cytosolic JC-1 monomers, merged images indicate the co-localization of JC-1 aggregates and monomers. (E) Quantitative assessment of JC-1 fluorescence. The results show the ratios of red to green JC-1 mean fluorescence intensities in different groups. Western blot analysis of (F) Mito Cyto c and (G) Cyto Cyt c levels. (H) Western blot analysis of cleaved caspase-3 levels. For all experiments, *P<0.05, **P<0.01 and ***P<0.001. The data are presented as the mean ± standard deviation. D-gal, D-galactose; 8-OHdG, 8-hydroxy-2'-deoxyguanosine; Mito Cyt c, mitochondrial cytochrome *c*; Cyto Cyt c, cytosolic cytochrome *c*; CD, common deletion; DMSO, dimethyl sulfoxide.

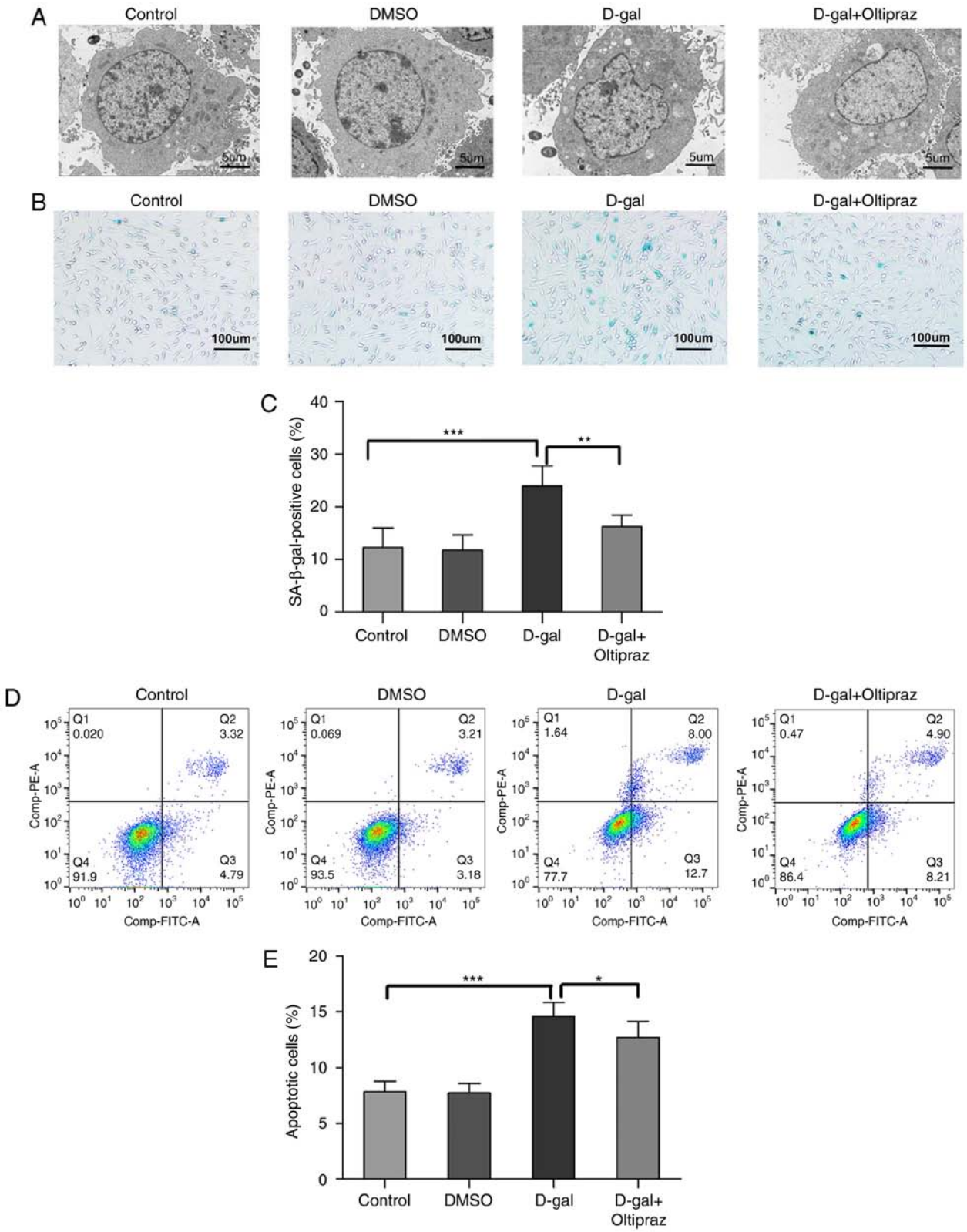

Figure 9. Oltipraz alleviates D-gal-induced damage, apoptosis and senescence in PC12 cells. (A) Representative images of transmission electron microscopy in the treated cells. (B) Representative images of senescence-associated β-galactosidase staining. (C) Percentages of cells positive for SA-β-gal staining. (D) Levels of apoptosis were measured in the treated cells using Annexin V-FITC/PI staining and analyzed by flow cytometry. (E) Quantitative presentation of apoptotic cells. For all experiments, *P<0.05, **P<0.01 and ***P<0.001. The data are presented as the mean ± standard deviation. D-gal, D-galactose; PI, propidium iodide; SA-β-gal, senescence-associated β-galactosidase.

cellular senescence. Therefore, decreased Nrf2-mediated antioxidant responses may induce mtDNA damage, apoptosis and degeneration in the auditory cortex, resulting in central presbycusis. The restoration of Nrf2 signaling activity may represent a potential therapeutic strategy for age-associated diseases, including central presbycusis.

Acknowledgements

Not applicable.

Funding

The present study was supported by grants from the National Natural Science Foundation of China (grant no. 81230021), the Major State Basic Research Development Program of China (973 Program; grant no. 2011CB504504) and the National Natural Science Foundation of China (grant no. 81670929).

Availability of data and materials

The analyzed datasets generated during the present study are available from the corresponding author on reasonable request.

Authors' contributions

YL, WK and WJK conceived and designed the experiments; YL, XZ, YH, HS, ZH, JY, HC, YS and XH performed the experiments; YL, WK and WJK analyzed the data; YL, YH, WK and WJK wrote the manuscript. All the authors have read and approved the final version of this manuscript.

Ethics approval and consent to participate

All procedures involving the care of animals were performed in accordance with the guidelines of the Care and Use of Laboratory Animals of the National Institutes of Health. The study protocol was approved by the Committee on the Ethics of Animal Experiments of HUST.

Patient consent for publication

Not applicable.

Competing interests

The authors declare that they have no competing interests.

References

1. Fetoni AR, Picciotti PM, Paludetti G and Troiani D: Pathogenesis of presbycusis in animal models: A review. Exp Gerontol 46: 413-425, 2011.
2. McCormack A and Fortnum H: Why do people fitted with hearing aids not wear them? Int J Audiol 52: 360-368, 2013.
3. Gates GA and Mills JH: Presbycusis. Lancet 366: 1111-1120, 2005.
4. Walton JP, Frisina RD and O'Neill WE: Age-related alteration in processing of temporal sound features in the auditory midbrain of the CBA mouse. J Neurosci 18: 2764-2776, 1998.
5. Gao X, Tao Y, Lamas V, Huang M, Yeh WH, Pan B, Hu YJ, Hu JH, Thompson DB, Shu Y, *et al*: Treatment of autosomal dominant hearing loss by in vivo delivery of genome editing agents. Nature 553: 217-221, 2018.
6. Zhang Y, Tang W, Ahmad S, Sipp JA, Chen P and Lin X: Gap junction-mediated intercellular biochemical coupling in cochlear supporting cells is required for normal cochlear functions. Proc Natl Acad Sci USA 102: 15201-15206, 2005.
7. He Z, Sun S, Waqas M, Zhang X, Qian F, Cheng C, Zhang M, Zhang S, Wang Y, Tang M, *et al*: Reduced TRMU expression increases the sensitivity of hair-cell-like HEI-OC-1 cells to neomycin damage in vitro. Sci Rep 6: 29621, 2016.
8. Menardo J, Tang Y, Ladrech S, Lenoir M, Casas F, Michel C, Bourien J, Ruel J, Rebillard G, Maurice T, *et al*: Oxidative stress, inflammation, and autophagic stress as the key mechanisms of premature age-related hearing loss in SAMP8 Mouse Cochlea. Antioxid Redox Signal 16: 263-274, 2012.
9. Uchida Y, Sugiura S, Sone M, Ueda H and Nakashima T: Progress and prospects in human genetic research into age-related hearing impairment. Biomed Res Int 2014: 390601, 2014.
10. Gates GA, Couropmitree NN and Myers RH: Genetic associations in age-related hearing thresholds. Arch Otolaryngol Head Neck Surg 125: 654-659, 1999.
11. Kinoshita M, Sakamoto T, Kashio A, Shimizu T and Yamasoba T: Age-related hearing loss in Mn-SOD heterozygous knockout mice. Oxid Med Cell Longev 2013: 325702, 2013.
12. Hensley K, Mhatre M, Mou S, Pye QN, Stewart C, West M and Williamson KS: On the relation of oxidative stress to neuroinflammation: Lessons learned from the G93A-SOD1 mouse model of amyotrophic lateral sclerosis. Antioxid Redox Signal 8: 2075-2087, 2006.
13. Harman D: Aging: A theory based on free radical and radiation chemistry. J Gerontol 10: 298-300, 1956.
14. Venugopal R and Jaiswal AK: Nrf1 and Nrf2 positively and c-Fos and Fra1 negatively regulate the human antioxidant response element-mediated expression of NAD(P)H:quinone oxidoreductase(1) gene. Proc Natl Acad Sci USA 93: 14960-14965, 1996.
15. Scandalios JG: Oxidative stress: Molecular perception and transduction of signals triggering antioxidant gene defenses. Braz J Med Biol Res 38: 995-1014, 2005.
16. Jiang H, Talaska AE, Schacht J and Sha SH: Oxidative imbalance in the aging inner ear. Neurobiol Aging 28: 1605-1612, 2007.
17. Tavanai E and Mohammadkhani G: Role of antioxidants in prevention of age-related hearing loss: A review of literature. Eur Arch Otorhinolaryngol 274: 1821-1834, 2017.
18. Liu L, Chen Y, Qi J, Zhang Y, He Y, Ni W, Li W, Zhang S, Sun S, Taketo MM, *et al*: Wnt activation protects against neomycin-induced hair cell damage in the mouse cochlea. Cell Death Dis 7: e2136, 2016.
19. Bratic A and Larsson NG: The role of mitochondria in aging. J Clin Invest 123: 951-957, 2013.
20. Pinto M and Moraes CT: Mechanisms linking mtDNA damage and aging. Free Radic Biol Med 85: 250-258, 2015.
21. Someya S and Prolla TA: Mitochondrial oxidative damage and apoptosis in age-related hearing loss. Mech Ageing Dev 131: 480-486, 2010.
22. Park CB and Larsson NG: Mitochondrial DNA mutations in disease and aging. J Cell Biol 193: 809-818, 2011.
23. Wang AL, Lukas TJ, Yuan M and Neufeld AH: Increased mitochondrial DNA damage and down-regulation of DNA repair enzymes in aged rodent retinal pigment epithelium and choroid. Mol Vis 14: 644-651, 2008.
24. Hebert SL, Lanza IR and Nair KS: Mitochondrial DNA alterations and reduced mitochondrial function in aging. Mech Ageing Dev 131: 451-462, 2010.
25. Markaryan A, Nelson EG and Hinojosa R: Quantification of the mitochondrial DNA common deletion in presbycusis. Laryngoscope 119: 1184-1189, 2009.
26. Yu J, Wang Y, Liu P, Li Q, Sun Y and Kong W: Mitochondrial DNA common deletion increases susceptibility to noise-induced hearing loss in a mimetic aging rat model. Biochem Biophys Res Commun 453: 515-520, 2014.
27. Dinkova-Kostova AT and Abramov AY: The emerging role of Nrf2 in mitochondrial function. Free Radic Biol Med 88: 179-188, 2015.
28. Niture SK, Khatri R and Jaiswal AK: Regulation of Nrf2-an update. Free Radic Biol Med 66: 36-44, 2014.
29. Cui X, Wang L, Zuo P, Han Z, Fang Z, Li W and Liu J: D-galactose-caused life shortening in Drosophila melanogaster and Musca domestica is associated with oxidative stress. Biogerontology 5: 317-325, 2004.
30. Ho SC, Liu JH and Wu RY: Establishment of the mimetic aging effect in mice caused by D-galactose. Biogerontology 4: 15-18, 2003.
31. Kong WJ, Wang Y, Wang Q, Hu YJ, Han YC and Liu J: The relation between D-galactose injection and mitochondrial DNA 4834 bp deletion mutation. Exp Gerontol 41: 628-634, 2006.
32. Sun HY, Hu YJ, Zhao XY, Zhong Y, Zeng LL, Chen XB, Yuan J, Wu J, Sun Y, Kong W and Kong WJ: Age-related changes in mitochondrial antioxidant enzyme Trx2 and TXNIP-Trx2-ASK1 signal pathways in the auditory cortex of a mimetic aging rat model: Changes to Trx2 in the auditory cortex. FEBS J 282: 2758-2774, 2015.

33. Willott JF: Effects of sex, gonadal hormones, and augmented acoustic environments on sensorineural hearing loss and the central auditory system: Insights from research on C57BL/6J mice. Hear Res 252: 89-99, 2009.
34. The National Academies Collection: Reports funded by National Institutes of Health. National Research Council Committee for the Update of the Guide for the Care and Use of Laboratory. Guide for the Care and Use of Laboratory Animals, 8th edition. National Academies Press (US), National Academy of Sciences, Washington, DC, 2011.
35. Ouahchi Y, Duclos C, Marie JP and Verin E: Implication of the vagus nerve in breathing pattern during sequential swallowing in rats. Physiol Behav 179: 434-441, 2017.
36. Louro TM, Matafome PN, Nunes EC, Xavier da Cunha F and Seiça RM: Insulin and metformin may prevent renal injury in young type 2 diabetic Goto-Kakizaki rats. Eur J Pharmacol 653: 89-94, 2011.
37. Zeng L, Yang Y, Hu Y, Sun Y, Du Z, Xie Z, Zhou T and Kong W: Age-related decrease in the mitochondrial sirtuin deacetylase Sirt3 expression associated with ROS accumulation in the auditory cortex of the mimetic aging rat model. PLoS One 9: e88019, 2014.
38. Wu X, Wang Y, Sun Y, Chen S, Zhang S, Shen L, Huang X, Lin X and Kong W: Reduced expression of Connexin26 and its DNA promoter hypermethylation in the inner ear of mimetic aging rats induced by d-galactose. Biochem Biophys Res Commun 452: 340-346, 2014.
39. Alves HN, da Silva AL, Olsson IA, Orden JM and Antunes LM: Anesthesia with intraperitoneal propofol, medetomidine, and fentanyl in rats. J Am Assoc Lab Anim Sci 49: 454-459, 2010.
40. Ferrari L, Turrini G, Rostello C, Guidi A, Casartelli A, Piaia A and Sartori M: Evaluation of two combinations of Domitor, Zoletil 100, and Euthatal to obtain long-term nonrecovery anesthesia in Sprague-Dawley rats. Comp Med 55: 256-264, 2005.
41. Yuan J, Zhao X, Hu Y, Sun H, Gong G, Huang X, Chen X, Xia M, Sun C, Huang Q *et al*: Autophagy regulates the degeneration of the auditory cortex through the AMPK-mTOR-ULK1 signaling pathway. Int J Mol Med 41: 2086-2098, 2018.
42. Nicklas JA, Brooks EM, Hunter TC, Single R and Branda RF: Development of a quantitative PCR (TaqMan) assay for relative mitochondrial DNA copy number and the common mitochondrial DNA deletion in the rat. Environ Mol Mutagen 44: 313-320, 2004.
43. Livak KJ and Schmittgen TD: Analysis of relative gene expression data using real-time quantitative PCR and the 2(-Delta Delta C(T)) method. Methods 25: 402-408, 2001.
44. Itahana K, Campisi J and Dimri GP: Methods to detect biomarkers of cellular senescence. In: Biological Aging: Methods and Protocols. Tollefsbol TO (ed). Humana Press, Totowa, NJ, pp21-31, 2007.
45. Ayala A, Muñoz MF and Argüelles S: Lipid peroxidation: production, metabolism, and signaling mechanisms of malondialdehyde and 4-hydroxy-2-nonenal. Oxid Med Cell Longev 2014: 360438, 2014.
46. Valavanidis A, Vlachogianni T and Fiotakis C: 8-hydroxy-2'-deoxyguanosine (8-OHdG): A critical biomarker of oxidative stress and carcinogenesis. J Environ Sci Health C Environ Carcinog Ecotoxicol Rev 27: 120-139, 2009.
47. Suzuki T and Yamamoto M: Molecular basis of the Keap1-Nrf2 system. Free Radic Biol Med 88: 93-100, 2015.
48. Lee J, Song K, Huh E, Oh MS and Kim YS: Neuroprotection against 6-OHDA toxicity in PC12 cells and mice through the Nrf2 pathway by a sesquiterpenoid from Tussilago farfara. Redox Biol 18: 6-15, 2018.
49. Sáez-Orellana F, Fuentes-Fuentes MC, Godoy PA, Silva-Grecchi T, Panes JD, Guzmán L, Yévenes GE, Gavilán J, Egan TM, Aguayo LG and Fuentealba J: P2X receptor overexpression induced by soluble oligomers of amyloid beta peptide potentiates synaptic failure and neuronal dyshomeostasis in cellular models of Alzheimer's disease. Neuropharmacology 128: 366-378, 2018.
50. Park HJ, Zhao TT, Lee KS, Lee SH, Shin KS, Park KH, Choi HS and Lee MK: Effects of (-)-sesamin on 6-hydroxydopamine-induced neurotoxicity in PC12 cells and dopaminergic neuronal cells of Parkinson's disease rat models. Neurochem Int 83-84: 19-27, 2015.
51. Zhang Y, Wang Z, Li X, Wang L, Yin M, Wang L, Chen N, Fan C and Song H: Dietary iron oxide nanoparticles delay aging and ameliorate neurodegeneration in drosophila. Adv Mater 28: 1387-1393, 2016.
52. Denisova NA, Cantuti-Castelvetri I, Hassan WN, Paulson KE and Joseph JA: Role of membrane lipids in regulation of vulnerability to oxidative stress in PC12 cells: Implication for aging. Free Radic Biol Med 30: 671-678, 2001.
53. Lee JS and Surh YJ: Nrf2 as a novel molecular target for chemoprevention. Cancer Lett 224: 171-184, 2005.
54. Evans MD, Dizdaroglu M and Cooke MS: Oxidative DNA damage and disease: Induction, repair and significance. Mutat Res 567: 1-61, 2004.
55. Andreollo NA, Santos EFd, Araújo MR and Lopes LR: Idade dos ratos versus idade humana: Qual é a relação? ABCD Arq Bras Cir Dig 25: 49-51, 2012.
56. Florczyk U, Łoboda A, Stachurska A, Józkowicz A and Dulak J: Role of Nrf2 transcription factor in cellular response to oxidative stress. Postepy Biochem 56: 147-155, 2010 (In Polish).
57. Jasper H: SKNy worms and long life. Cell 132: 915-916, 2008.
58. Kubben N, Zhang W, Wang L, Voss TC, Yang J, Qu J, Liu GH and Misteli T: Repression of the antioxidant NRF2 pathway in premature aging. Cell 165: 1361-1374, 2016.
59. Kobayashi A, Kang MI, Watai Y, Tong KI, Shibata T, Uchida K and Yamamoto M: Oxidative and electrophilic stresses activate Nrf2 through inhibition of ubiquitination activity of Keap1. Mol Cell Biol 26: 221-229, 2006.
60. Kim HJ and Vaziri ND: Contribution of impaired Nrf2-Keap1 pathway to oxidative stress and inflammation in chronic renal failure. Am J Physiol Renal Physiol 298: F662-F671, 2010.
61. Chen H and Tang J: The role of mitochondria in age-related hearing loss. Biogerontology 15: 13-19, 2014.
62. de Souza-Pinto NC, Hogue BA and Bohr VA: DNA repair and aging in mouse liver: 8-oxodG glycosylase activity increase in mitochondrial but not in nuclear extracts. Free Radic Biol Med 30: 916-923, 2001.
63. Souza-Pinto NC, Croteau DL, Hudson EK, Hansford RG and Bohr VA: Age-associated increase in 8-oxo-deoxyguanosine glycosylase/AP lyase activity in rat mitochondria. Nucleic Acids Res 27: 1935-1942, 1999.
64. Mecocci P, MacGarvey U and Beal MF: Oxidative damage to mitochondrial DNA is increased in Alzheimer's disease. Ann Neurol 36: 747-751, 1994.
65. Wang AL, Lukas TJ, Yuan M and Neufeld AH: Age-related increase in mitochondrial DNA damage and loss of DNA repair capacity in the neural retina. Neurobiol Aging 31: 2002-2010, 2010.
66. Cividini F, Scott BT, Dai A, Han W, Suarez J, Diaz-Juarez J, Diemer T, Casteel DE and Dillmann WH: O-GlcNAcylation of 8-Oxoguanine DNA glycosylase (Ogg1) impairs oxidative mitochondrial DNA lesion repair in diabetic hearts. J Biol Chem 291: 26515-26528, 2016.
67. Dinkova-Kostova AT and Talalay P: NAD(P)H:Quinone acceptor oxidoreductase 1 (NQO1), a multifunctional antioxidant enzyme and exceptionally versatile cytoprotector. Arch Biochem Biophys 501: 116-123, 2010.
68. Bauer AK, Faiola B, Abernethy DJ, Marchan R, Pluta LJ, Wong VA, Roberts K, Jaiswal AK, Gonzalez FJ, Butterworth BE, *et al*: Genetic susceptibility to benzene-induced toxicity: Role of NADPH: Quinone oxidoreductase-1. Cancer Res 63: 929, 2003.
69. True AL, Olive M, Boehm M, San H, Westrick RJ, Raghavachari N, Xu X, Lynn EG, Sack MN, Munson PJ, *et al*: Heme oxygenase-1 deficiency accelerates formation of arterial thrombosis through oxidative damage to the endothelium, which is rescued by inhaled carbon monoxide. Circ Res 101: 893-901, 2007.
70. Williams MD, Van Remmen H, Conrad CC, Huang TT, Epstein CJ and Richardson A: Increased oxidative damage is correlated to altered mitochondrial function in heterozygous manganese superoxide dismutase knockout mice. J Biol Chem 273: 28510-28515, 1998.
71. Gaziev AI, Abdullaev S and Podlutsky A: Mitochondrial function and mitochondrial DNA maintenance with advancing age. Biogerontology 15: 417-438, 2014.
72. Onken B and Driscoll M: Metformin induces a dietary restriction-like state and the oxidative stress response to extend C. elegans healthspan via AMPK, LKB1, and SKN-1. PLoS One 5: e8758, 2010.
73. Chen X, Zhao X, Cai H, Sun H, Hu Y, Huang X, Kong W and Kong W: The role of sodium hydrosulfide in attenuating the aging process via PI3K/AKT and CaMKKβ/AMPK pathways. Redox Biol 12: 987-1003, 2017.
74. Zhao XY, Sun JL, Hu YJ, Yang Y, Zhang WJ, Hu Y, Li J, Sun Y, Zhong Y, Peng W, *et al*: The effect of overexpression of PGC-1α on the mtDNA4834 common deletion in a rat cochlear marginal cell senescence model. Hear Res 296: 13-24, 2013.